



## Very Forward Jets as A Probe for Low-x Parton Evolution

Mahmoud Attia Mahmoud<sup>1\*</sup>, Ralf Ulrich<sup>2</sup>, A. Elabd<sup>1</sup>, N. Rashed<sup>3</sup>, Yasser Mohammed<sup>3</sup>

<sup>1</sup>Reactor Physics Department, Egyptian Atomic Energy Authority, Egypt

<sup>2</sup>Center for High Energy Physics(CHEP-FU)

<sup>3</sup>Physics Department, Fayoum University, Fayoum City, Egypt

**J**ETS in high energy hadron-hadron collisions emerge from the interaction of partons at high transverse momenta. The dynamic of hadron jets in proton-proton collisions provides essential information about Parton scattering. The studying of very forward dijet events is very important to enhance the sensitivity to very small-x Parton dynamics. Azimuthal angle decorrelation is a sensitive probe for details of QCD radiation in hard parton scattering. A study of azimuthal angle decorrelations of Mueller-Navelet and inclusive dijet cross-section in proton-proton collisions were performed for jets with  $p_T > 5$  GeV and different values of pseudorapidity  $\Delta\eta$  using different Monte Carlo generators samples at  $\sqrt{s} = 13$  TeV. This work using various Monte-Carlo generators to make comparison that allows distinguishing among various Monte-Carlo generators and their tunes. Monte Carlo generator samples used are Pythia8 CUETP8M1, Pythia8 MBR and EPOS-LHC. For each value of pseudorapidity  $\Delta\eta$ , the dijet cross-section and  $\Delta\phi$  distributions for MN dijets are measured.

**Keywords :** Forward dijet event, Azimuthal angle decorrelation, Mueller-Navelet, MN dijets

### Introduction

Jets in high energy hadron-hadron collisions emerge from the interaction of partons at high transverse momenta. The cross-section of jet production can be described as a series in perturbative quantum chromodynamics. Inclusive jet production measured over a wide range in transverse momenta and as a function of rapidity,  $y$  is well described by predictions from pQCD and used to constrain the Parton densities [1,2]. The production of dijets has also been measured at highest energies, and a good description by theory has been obtained [3, 4].

QCD is well tested in hard processes, and the data are successfully described by perturbative QCD calculations within the framework of collinear factorization and Dokshitzer-Gribov-Lipatov-Altarelli-Parisi (DGLAP) evolution equations [5–6]. The dynamic of hadron jets in proton-proton collisions provides essential information about Parton scattering. Perturbative QCD at the leading order (LO) predicts the

production of a back-to-back in azimuthal angle  $\phi$  jets in hard parton scattering. Azimuthal angles decorrelations of jets are due to higher-order effects described by the parton showering in the initial and final states of the scattering process.

When the separation in pseudorapidity ( $\Delta\eta$ ) between the jets is very small or, particular vast regions of phase space are probed. At small pseudorapidity separation between jets, both jets move in a similar direction with a small invariant dijet mass. The dijet system has to be balanced by one or more additional jets. A different scenario is obtained at large  $\Delta\eta$ , when the jets are opposite in  $\eta$ , and a large dijet invariant mass is obtained. In this region, additional soft partons can be emitted between the jets (BFKL [7–9] predicts an increase of radiation for increasing  $\Delta\eta$ ). Previous measurements of dijet production at large rapidity separation [10,11] are reasonably well described by Monte Carlo event simulation or calculations at next to leading order in pQCD, and no significant sign for BFKL effects is observed.

\*Corresponding author: e-mail: mahmoud.mohamed@cern.ch

DOI :10.21608/EJPHYSICS.2022.113012.1073

Received : 30/12/2021; accepted : 27/2/2022

©2022 National Information and Documentaion Center (NIDOC)

The presented measurements have initially been motivated by a search for BFKL effects (Mueller-Navelet jets [12]). Still, they are also interested in a more general sense of how well the differential cross-section for high transverse momentum jets is described with the different theoretical approaches. Is there a region where the available calculations fail to describe the measurement. The region of large  $\Delta\eta$  is of importance since it constitutes a non-reducible background for vector-boson-fusion measurements. The region of small  $\Delta\eta$  is of relevance because of its non-reducible background to heavy boosted objects.

In this work several observables connected to azimuthal angle decorrelation and dijet cross section of Mueller-Navelet jets are studied. The most straightforward observable is the distribution of azimuthal angle difference,  $\Delta\phi$ , between Mueller-Navelet jets. A study of a azimuthal angle decorrelations of Mueller-Navelet and inclusive dijet cross section in proton-proton collisions was performed for jets with  $>5$  GeV and different values of pseudorapidity  $|\eta|$  using data collected with the CMS detector at the LHC in 2015 at  $\sqrt{s} = 13$  TeV.

#### Monte Carlo (MC) Samples

Table 1 contains some Monte Carlo (MC) samples used for this work. The PYTHIA Monte Carlo generator [13, 14] uses the Donnachie-Landshoff parameterization [15] for the total hadronic cross-section. Various models may be used for the elastic and diffractive cross-section (unless stated differently, the default Schuler-Sjo strand model [16, 17] is used). In contrast, the remainder of the total cross-section is used to normalize the nondiffractive part, which is generated through low- “minimum-bias” processes. Event samples are generated with different diffractive and underlying event tunes: the Z2\* [18] tune is used for the PYTHIA6 (version 6.426) sample, while PYTHIA8 (version 8.205) samples are generated with the Monash [19], CUETM1 [20], Donnachie-Landshoff (DL) [21], and Minimum-Bias-Rockefeller (MBR) [22] tunes. These tunes differ in their parameters used to describe initial and final

**TABLE 1. Summary of Monte Carlo samples with some of the main parameters.**

MC generator	Number Of Events
Pythia8 Tune MBR	4862000
Pythia8 Tune CUETP8M1	4917500
EPOS-LHC	4978400

state Parton showers, multi-party interactions, and hadronization. The DL and MBR tunes also use an alternative diffraction model, with the MBR model based on a phenomenological renormalized-Regge-theory model [22, 23].

The EPOS-LHC and event generator are partially designed to “bridge the gap” between collider and cosmic-ray physics by simultaneously providing descriptions for both event classes. EPOS-LHC is based on RGT (Regge-Gribov theory)

#### Event Selection

This analysis is based on ppcollisionMC generator models at 13 TeV. The transverse jet momenta that all jets must have  $> 5$  GeV, but for pseudorapidity, there are three states:

1.  $\eta_1 > 0$  for the first jet, and  $< 0$  for the second jet where  $\Delta\eta = |\eta_1 - \eta_2|$ .
2.  $\eta_1 > 0$ , and another jet in the CASTOR detector area.
3.  $\eta_1 > 3$ , where it is in HF range, the second jet has  $\eta_2 < -4.25$ .

For each value for pseudorapidity, there is one plot describing the cross-section and azimuthal decorrelations of dijet.

#### Jet Selection

In order to obtain Mueller-Navelet type jets, the following criteria are applied. Jets were reconstructed using anti- $k_r$  algorithm [25] with cone radius of  $R = 0.4$ .

- The events have been selected which have jets with  $p_T > 5$  GeV.
- Select two jets for each event with the largest rapidity separation and tag them most forward and most backward jets.

#### $\Delta\phi$ Distribution

The azimuthal angle differences  $\Delta\phi$  and dijet cross-section  $\Delta\eta$  are plotted in Fig. 1 and Fig. 2 for the first state (section 2), Fig. 3 and Fig. 4 for the second state and Fig. 5 and Fig. 6 for the third. For each value  $\eta$  there is two plots for the cross-section and azimuthal decorrelations of dijet. As shown in Fig. 1, it describes the dijet cross-section in which the two jets have  $>5$  GeV, and  $\eta_1 > 0$  for the first jet, and  $\eta_2 < 0$  for the second jet where  $\Delta\eta = |\eta_1 - \eta_2|$ . The peak delta-eta is around 1 for these jets. The dijet azimuthal decorrelations is shown in Fig. 2. This was the first state of measuring the dijet cross-section.

The second state describes the correlation between one jet having  $\eta_1 > 0$  and another in the CASTOR detector. The peak delta-eta is around 5.5 for these jets, as shown in Fig. 3, which shows

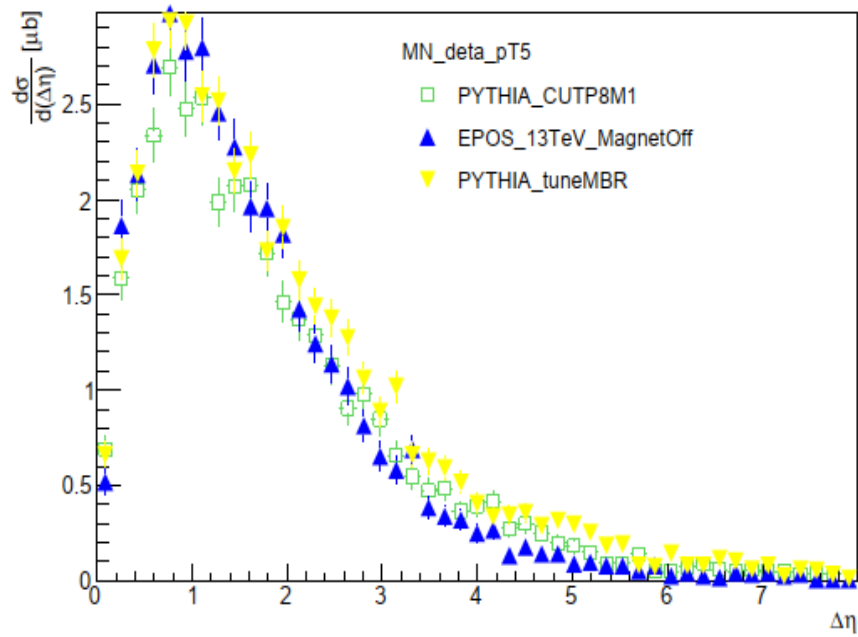


Fig. 1. Inclusive dijet cross section as a function of  $\Delta\eta$  with both jets with  $P_T > 5$  GeV and  $\Delta\eta > 0$ . It shows comparison for the three MC models Pythia8 TuneCUETP8M1, Pythia8 TuneMBR and Epos LHC.

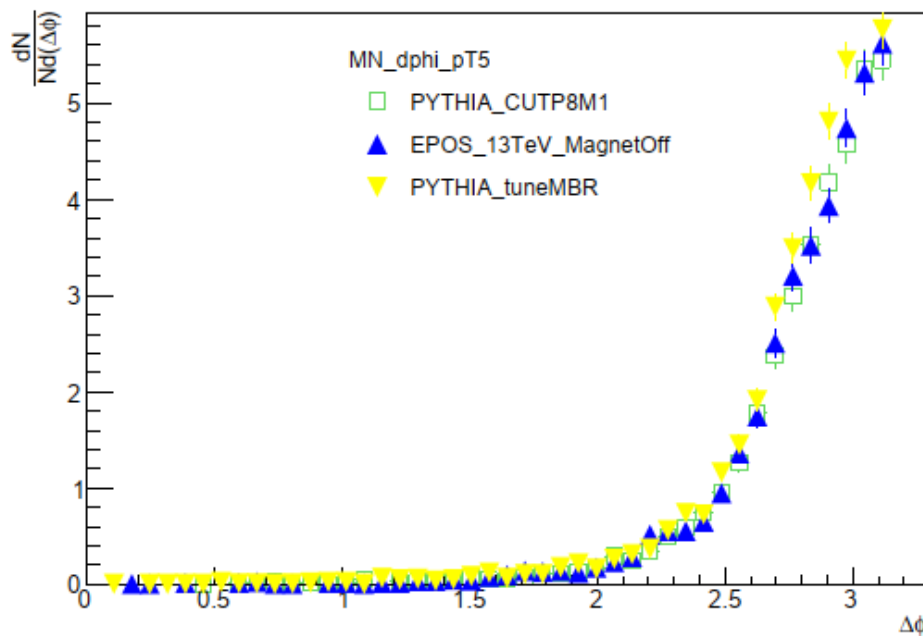
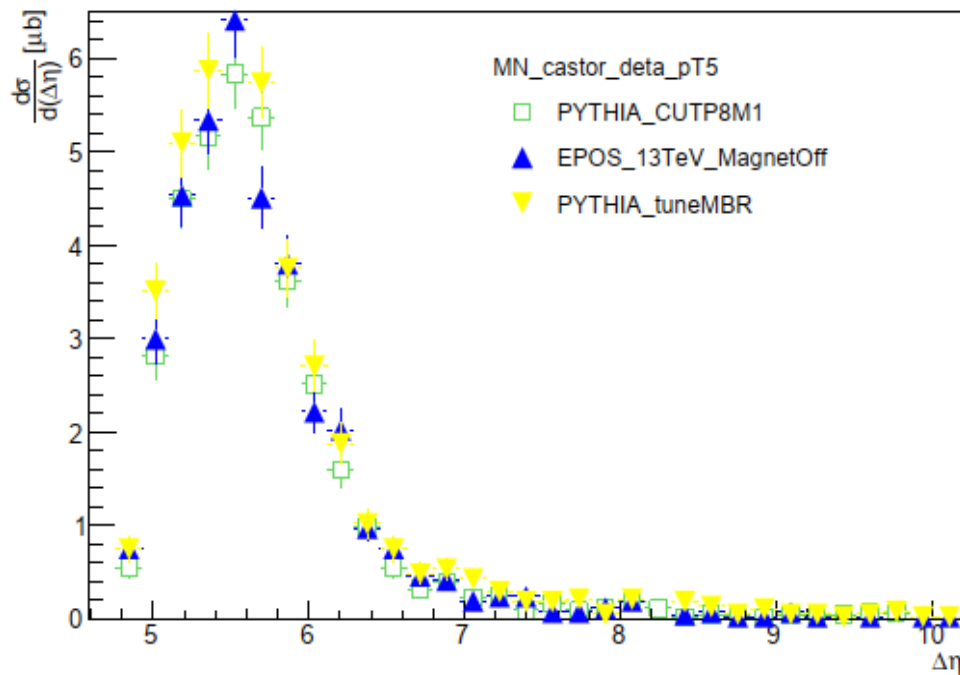
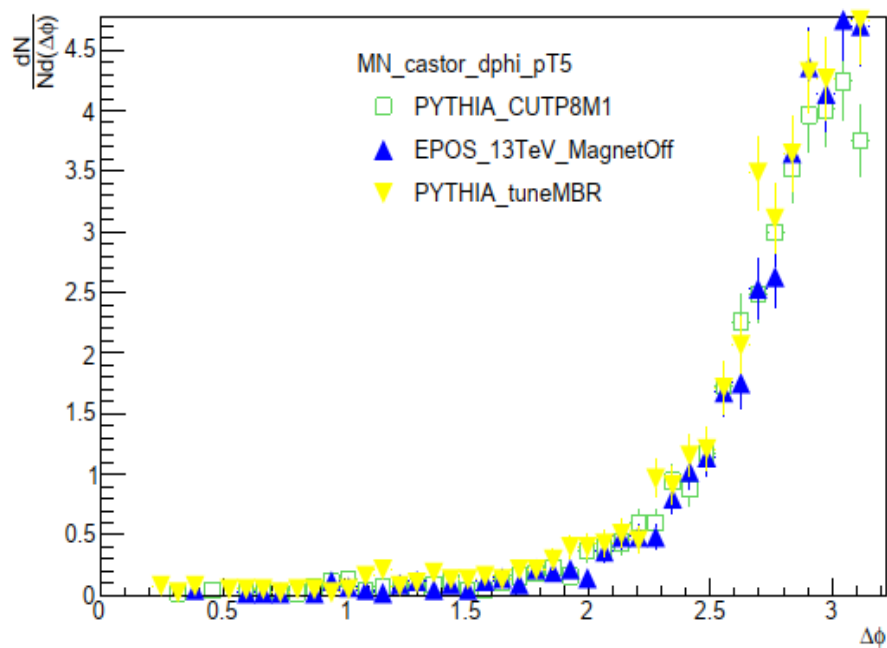


Fig. 2. Comparison of shape of  $\Delta$  distributions for dijets for Pythia8 TuneCUETP8M1, Pythia8 TuneMBR and Epos LHC. With  $\sqrt{s} = 13$  GeV and  $\Delta\eta > 0$ .



**Fig. 3.** Dijet cross section as a function of  $\Delta$  with both jets with  $> 5$  GeV and  $\Delta\eta > 4.5$ , that one jet in the positive side, and the second one in CASTOR area. It shows comparison for the three MC models Pythia8 TuneCUETP8M1, Pythia8 TuneMBR and Epos LHC



**Fig. 4.** Comparison of shape of  $\Delta$  distributions for dijets that one jet in the positive side, and the second one in CASTOR area. for Pythia8 TuneCUETP8M1, Pythia8 TuneMBR and Epos LHC. With GeV and  $\Delta\eta > 4.5$ .

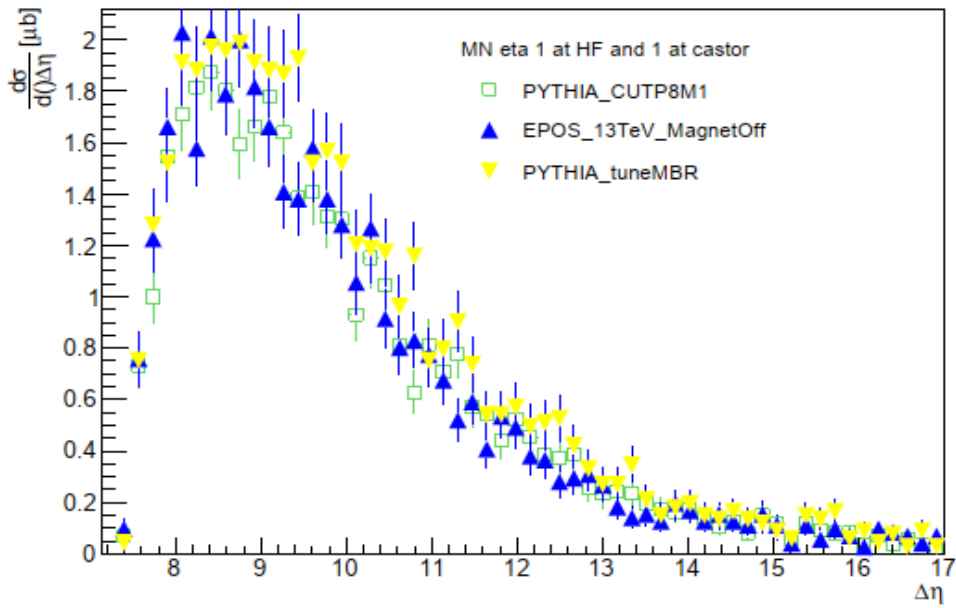


Fig. 5. MNdijet cross section as a function of  $\Delta$  with both jets with  $> 5$  GeV and  $\Delta\eta > 7.25$ . It is back-to-back dijet cross section, for Pythia8 TuneCUETP8M1, Pythia8 TuneMBR and Epos LHC.

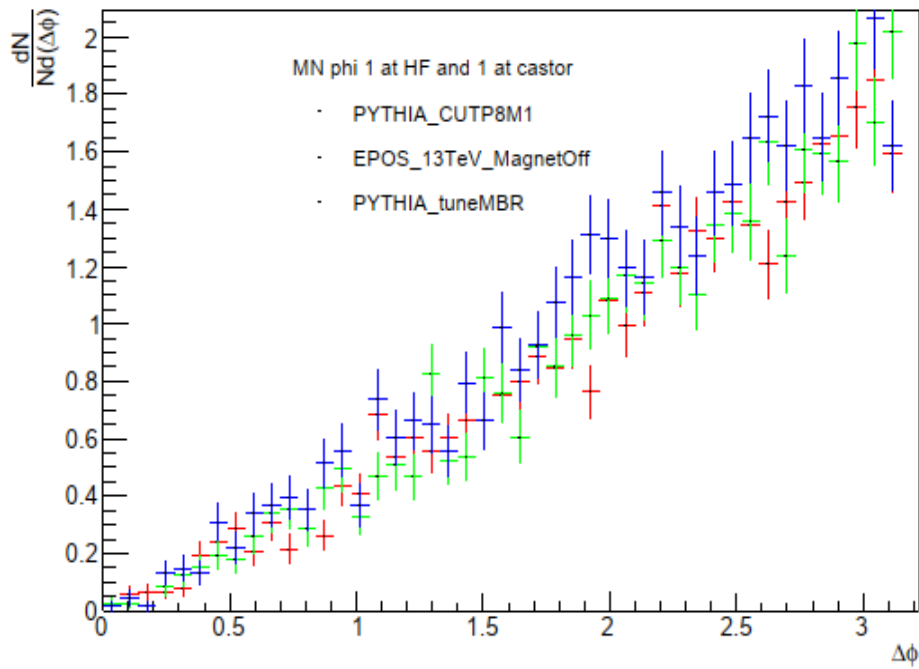


Fig. 6. Comparison of shape of  $\Delta$  distributions for MNdijets for Pythia8 TuneCUETP8M1, Pythia8 TuneMBR and Epos LHC, with  $> 5$  GeV and  $\Delta\eta > 7.25$ . It is Back-to-back dijet azimuthal decorrelations.

the dijet cross-section, and figure(4) shows dijet azimuthal decorrelations. The delta-phi remains almost unaffected.

The third state describes the correlation between one jet has  $\eta_1 > 3$ , where it is in HF range, the second jet has  $\eta_2 < -4.25$ , the last range it combines HF to CASTOR detector in the negative side, this is shown in Fig. 5 and Fig. 6. For this configuration, the peak delta-eta is almost 9. There is significant azimuthal decorrelation observed here.

### Discussion

As shown from the above figures, several observables are connected to azimuthal angle decorrelation  $\Delta\phi$  and dijet cross-section  $\Delta\eta$  of Mueller-Navelet jets. A study of azimuthal angle decorrelations of Mueller-Navelet and inclusive dijet cross section in proton-proton collisions was performed for jets (see sections 3 and 4) with  $p_{\perp}(T) > 5$  GeV and different values of pseudorapidity  $\Delta\eta$  using data collected with the CMS detector at the LHC in 2015 at  $\sqrt{s} = 13$  TeV. The azimuthal correlation  $\Delta\phi$  and dijet cross-section  $\Delta\eta$  of Mueller-Navelet jets are measured in three states:

1. The first jet has  $\eta < 0$ , and the other has  $\eta > 0$ .
2. The first jet has  $\eta > 0$ , and the other has a CASTOR detector.
3. The first jet at HF (+ev direction), and the other at CASTOR detector.

The azimuthal angle differences  $\Delta\phi$  and dijet cross-section  $\Delta\eta$  are plotted in Fig. 1 and Fig. 2 for the first state, the peak delta-eta is around 1 for these jets. Figure 3 and Fig. 4 for the second state, where the peak delta-eta is around 5.5 for these jets, and the delta-phi remains almost unaffected. Figure 5 and Fig. 6 for the third state, the peak delta-eta is almost 9. There is significant azimuthal decorrelation observed here.

### Summary

For the measurement of dijet production as a function of the separation in pseudorapidity at  $\sqrt{s} = 13$  TeV was done, and dijet azimuthal decorrelations are also done. When the separation in pseudorapidity ( $\Delta\eta$ ) between the jets is very small or very large special regions of phase space are probed. At small pseudorapidity separation between jets, both jets move in a similar direction with a small invariant dijet mass. The dijet system has to be balanced by one or more additional jets. A different scenario is obtained at large  $\Delta\eta$  when the jets are opposite in  $\eta$ , and a large dijet invariant

mass is obtained. In this region, additional soft partons can be emitted between the jets (BFKL predicts an increase of radiation for increasing  $\Delta\eta$ ). The presented measurements were originally motivated by searching for BFKL effects (Mueller-Navelet jets).

The azimuthal correlation between central and forward jets has been measured in proton-proton collisions at the LHC recorded with the CMS detector at a centre-of-mass energy of 13 TeV is done in three states as follow:

1. The first jet has  $\eta < 0$ , and the other has  $\eta > 0$ .
2. The first jet has  $\eta > 0$ , and the other has a CASTOR detector.
3. The first jet at HF (+ev direction), and the other at CASTOR detector.

All of these studies were done with  $p_{\perp} > 5$  GeV.

### References

1. ATLAS Collaboration, "Measurement of the inclusive jet cross section in pp collisions at  $\sqrt{s} = 2.76$  TeV and comparison to the inclusive jet cross section at  $\sqrt{s} = 7$  TeV using the ATLAS detector", *Eur. Phys. J. C* **73** (2013), no. 8, 2509, doi:10.1140/epjc/s10052-013-2509-4, arXiv:1304.4739
2. CMS Collaboration, "Measurement of the inclusive production cross sections for forward jets and forward jet events with one forward and one central jet in pp collisions at  $\sqrt{s} = 7$  TeV", *Journal of High Energy Physics* 2012 (8, 2012) doi:10.1007/JHEP06(2012)036.
3. CMS Collaboration, "Dijet azimuthal decorrelations in pp collisions at  $\sqrt{s} = 7$  TeV", *Phys. Rev. Lett.* **106** (2011) 122003, doi:10.1103/PhysRevLett.106.122003, 216 arXiv:1101.5029.
4. ATLAS Collaboration, "Measurement of dijet azimuthal decorrelations in pp collisions at  $\sqrt{s} = 7$  TeV", *Phys. Rev. Lett.* **106** (2011) 172002, 219 doi:10.1103/PhysRevLett.106.172002, arXiv:1102.2696
5. V.N. Gribov, L.N. Lipatov, "Deep inelastic e p scattering in perturbation theory", *Sov. J. Nucl. Phys.* **15** (1972) 438–450.
6. Y.L. Dokshitzer, "Calculation of the Structure Functions for Deep Inelastic Scattering and e+ e- Annihilation by Perturbation Theory in Quantum Chromodynamics", *Sov. Phys. JETP* **46** (1977) 641–653.
7. E.A. Kuraev, L.N. Lipatov, V.S. Fadin, "Multi-Reggeon Processes in the Yang-Mills Theory",

- Sov. Phys. JETP* **44** (1976) 443–450.
8. E.A. Kuraev, L.N. Lipatov, V.S. Fadin, “The Pomeron Singularity in Nonabelian Gauge Theories”, *Sov. Phys. JETP* **45** (1977) 199–204.
  9. I.I. Balitsky, L.N. Lipatov, “The Pomeron Singularity in Quantum Chromodynamics”, *Sov. J. Nucl. Phys.* **28** (1978) 822–829.
  10. CMS Collaboration, “Dijet Azimuthal Decorrelations in pp Collisions at = 7 TeV”, *Phys. Rev. Lett.* **106** (Jan, 2011) 122003. 28 p.
  11. CMS Collaboration Collaboration, “Azimuthal decorrelation of jets widely separated in rapidity in pp collisions at = 7 TeV”, arXiv:1601.06713. , submitted to *J. High Energy Phys.*
  12. A. H. Mueller and H. Navelet, “An inclusive minijet cross section and the bare pomeron in QCD”, *Nuclear Physics, B* **282** (1987) 727–744, doi:10.1016/0550-3213(87)90705-X.
  13. T. Sjostrand, S. Mrenna, and P. Z. Skands, “PYTHIA 6.4 Physics and Manual”, *JHEP* **05382** (2006) 026, doi:10.1088/1126-6708/2006/05/026, arXiv:hep-ph/0603175.
  14. T. Sjostrand, S. Mrenna, and P. Z. Skands, “A Brief Introduction to PYTHIA 8.1”, *Comput. Phys. Commun.* **178** (2008) 852–867, doi:10.1016/j.cpc.2008.01.036, arXiv:0710.3820.386
  15. A. Donnachie and P. V. Landshoff, “Total cross-sections”, *Phys. Lett.* **B296** (1992) 227–232, doi:10.1016/0370-2693(92)90832-O, arXiv:hep-ph/9209205.
  16. G.A. Schuler and T. Sjostrand, “Towards a complete description of high-energy photoproduction”, *Nucl. Phys.* **B407** (1993) 539–605, doi:10.1016/0550-3213(93)90091-3.
  17. G. A. Schuler and T. Sjostrand, “Hadronic diffractive cross-sections and the rise of the total cross-section”, *Phys. Rev.* **D49** (1994) 2257–2267, doi:10.1103/PhysRevD.49.2257.
  18. CMS Collaboration, “Study of the underlying event at forward rapidity in pp collisions at = 0.9, 2.76, and 7 TeV”, *JHEP* **04** (2013) 072, doi:10.1007/JHEP04(2013)072, arXiv:1302.2394.
  19. P. Skands, S. Carrazza, and J. Rojo, “Tuning PYTHIA 8.1: the Monash 2013 Tune”, *Eur. Phys. J.* **C74** (2014), no. 8, 3024, doi:10.1140/epjc/s10052-014-3024-y, arXiv:1404.5630.400.
  20. CMS Collaboration, “Event generator tunes obtained from underlying event and multiparton scattering measurements”, arXiv:1512.00815.
  21. A. Donnachie and P. V. Landshoff, “Elastic Scattering and Diffraction Dissociation”, *Nucl. Phys.* **B244** (1984) 322, doi:10.1016/0550-3213(84)90315-8. [,813(1984)].
  22. R. Ciesielski and K. Goulianos, “MBR Monte Carlo Simulation in PYTHIA8”, *PoS ICHEP* **2012** (2013) 301, arXiv:1205.1446.
  23. K. A. Goulianos, “Hadronic diffraction: Where do we stand?”, in *Results and perspectives in particle physics. Proceedings, 18<sup>th</sup> Rencontres de Physique de la Vallée d’Aoste, La Thuile, Italy, February 29-March 6, 2004*, pp. arXiv:hep-ph/0407035.
  24. K. A. Goulianos, “Diffraction in QCD”, in *Corfu Summer Institute on Elementary Particle Physics (Corfu 2001) Corfu, Greece, August 31-September 20, 2002*. arXiv:hep-ph/0203141.
  25. G. M. Cacciari and G. Soyez, “The anti-kt jet clustering algorithm”, *JHEP* **04** (2008) S08004.



